



Open Archive Toulouse Archive Ouverte (OATAO)

OATAO is an open access repository that collects the work of Toulouse researchers and makes it freely available over the web where possible.

This is an author-deposited version published in: <http://oatao.univ-toulouse.fr/>
Eprints ID: 3845

To link to this article: DOI: 10.1007/s11664-008-0571-8
URL: <http://dx.doi.org/10.1007/s11664-008-0571-8>

To cite this version: Chasserio, N. and Guillemet-Fritsch, Sophie and Lebey, Thierry and DAGDAG, S. (2009) *Ceramic Substrates for High-temperature Electronic Integration*. Journal of Electronic Materials, vol. 38 (n° 1). pp. 164-174. ISSN 0361-5235

Any correspondence concerning this service should be sent to the repository administrator: staff-oatao@inp-toulouse.fr

Ceramic Substrates for High-temperature Electronic Integration

N. CHASSERIO,¹ S. GUILLEMET-FRITSCH,¹ T. LEBEY,² and
S. DAGDAG^{3,4}

1.—Centre Inter-universitaire de Recherche et d'Ingénierie des Matériaux-CIRIMAT-Bât. 2R1, 118 Route de Narbonne, 31077 Toulouse Cedex 04, France. 2.—Laboratoire LAPLACE, Université Paul Sabatier. Bât. 3R3, 118, Route de Narbonne, 31062 Toulouse Cedex 9, France. 3.—Power Electronics Associated Research Laboratory, ALSTOM Transport, Rue du Docteur Guinier, 65 600 Semeac, France. 4.—e-mail: selim.dagdag@transport.alstom.com

One of the most attractive ways to increase power handling capacity in power modules is to increase the operating temperature using wide-band-gap semiconductors. Ceramics are ideal candidates for use as substrates in high-power high-temperature electronic devices. The present article aims to determine the most suitable ceramic material for this application.

Key words: High-temperature electronics, passive component, system integration, packaging, ceramic substrate

INTRODUCTION

The commercial availability of field-effect transistors made of silicon carbide (SiC-JFET or MOS-FET) has enabled studies to be initiated on the industrial development of power converters working at ambient temperatures exceeding 200°C. In aeronautic or automotive applications, the replacement of mechanical or hydraulic systems by electronic devices would result in increased performance and reduced weight of the system. However such novel designs would imply placing electronics and power electronics devices near the actuators or close to the engine—locations resulting in harsh environmental constraints for the device, involving extreme thermal excursions. The availability of high-temperature technology would enable spectacular gains in terms of accuracy, reduction of clutter, and optimization of efficiency. Classically a power device is a stack of several materials (semiconductors, ceramics, metallization, etc.). This combination is then fastened to a baseplate. The resulting complex and heterogeneous structure is subjected to a large number of stresses when in service. New power electronic

devices designed for operation at high temperatures would require extensive alterations, affecting their entire environment, such as the passivation, encapsulation, and substrates.^{1–3} This therefore requires adaption of the technological choices to the critical environmental constraints, and particularly the temperature ones. This also implies modification of most of the converter components (active and passive) for an environment where the ambient temperature can easily exceed 200°C, as is usually studied.⁴

With the aim of developing power converters that can operate safely at an ambient temperature of 300°C, this article focuses on one part of the assembly—the substrate. The substrate has several functions, including ensuring electrical insulation between the active components and the baseplate (which is generally grounded) while favoring the removal of losses generated by the dies (during both switching and conduction periods). Even though its thermal conductivity is of primary importance, other properties have to be taken into account. Previous studies³ have shown that the main causes of failure result from thermomechanical aging or physicochemical stresses. The substrate (the elementary part) must therefore have a coefficient of thermal expansion (CTE) close to those of the other parts of the whole assembly. Chemical stability of the materials with increasing temperature must also be ensured. Regarding its electrical properties,

the substrate must present high resistivity to reduce leakage current, a high dielectric strength to withstand the voltage, and a low dielectric constant to limit the common-mode capacitance. Lastly, to resist the constraints of handling, its mechanical strength must also be as high as possible.

For the present investigation, the targeted ambient temperature is 300°C, although hot spots up to 350°C to 400°C are possible. Such increases of temperature depend on the packaging technology and on the thermal management of the power devices. Therefore, the substrates' properties have to be characterized up to 450°C to 500°C. Taking into account the aforementioned requirements, metal-insulator-semiconductor systems can be dismissed due to their low electrical resistivity. On the other hand, polymers are not serious candidates since their behavior in this high-temperature range is inappropriate. Considering the required specifications, ceramic substrates are the only suitable candidates. Alumina, boron nitride, aluminum nitride, and silicon nitride are the most suitable ceramics due to their high thermal conductivity. Despite its excellent properties, beryllium oxide is not used because of its toxicity. Since the mid 1980s direct bonded copper (DBC) substrates have increasingly been used in power electronics. The reason why Al₂O₃ and AlN-DBC have become the preferred industry power substrates is their performance and competitive prices. However their properties at temperatures higher than 200°C still need to be evaluated and/or new materials envisaged. The best compromise between their various properties has to be reached not only to optimize and to increase the final performance of the converter but also to guarantee reliability.

This article presents the results of various characterizations (structural, microstructural, mechanical, thermal, and electrical) of alumina, boron nitride, aluminum nitride, and silicon nitride and aims to establish the best candidate among these materials for the application described. It also reports a large study of the behavior of these ceramic substrates over a high-temperature range reaching 500°C. In the first part, the general properties of the ceramics tested are introduced. Then, the different characterization methods are presented. The results for the different materials under study are then given and discussed.

CERAMIC SUBSTRATES

Various ceramic materials have been envisaged for this application, namely alumina, aluminum nitride, boron nitride, and silicon nitride. We first recall their general properties.

Alumina

Alumina is commonly used in power applications since it is the cheapest material for use as a substrate. Its physical characteristics mainly depend on its purity and its density. Samples under study are in the form of 50 mm × 50 mm × 0.635 mm plates (manufacturer 1, purity 99.6%).

Aluminum Nitride

Compared to alumina, AlN offers a significant increase in thermal performance for power circuit designers. However, its properties can vary greatly since the process of fabrication can change from one supplier to another (especially the kind and the amount of additive used). Two types of AlN have been tested in this article (AlN1 manufacturer 2 and AlN2 manufacturer 3). The samples were the same sizes as the alumina plates.

Boron Nitride

Boron nitride is expected to have a thermal conductivity higher than that of alumina, with a lower CTE. For these reasons, this material may substitute for alumina. In this article two thicknesses and two dimensions were studied namely: 50 mm × 50 mm × 0.635 mm and 50 mm × 50 mm × 1.67 mm (manufacturer 4, purity >95%).

Silicon Nitride

Si₃N₄ substrates present high mechanical resistance. This could be of considerable interest for reliability (particularly for thermomechanical aging) despite its low thermal conductivity (Table I). The dimensions of the Si₃N₄ plates studied were 50 mm × 50 mm × 0.635 mm (manufacturer 6).

The most commonly reported physical characteristics of these materials, including the supplier's values specified in the following, are given in Table I. The large dispersion of values observed in some cases is mainly due to the different processes

Table I. Physical Characteristics of the Materials under Study at Room Temperature

	Thermal Conductivity (W/m K)	CTE (10⁻⁶/°C)	Flexural Strength (MPa)	Dielectric Strength (kV/mm)
Alumina	26–35	6.8–9	300–400	10–20
Boron nitride	20–60	0.1–6	20–90	40–200
Aluminum nitride	150–180	4.3–6.2	300–350	14–17
Silicon nitride	20–30	2.6–3.6	500–800	10–14

and/or additives used by the different suppliers during the synthesis of the materials.

EXPERIMENTAL

The main analytical techniques used investigated the electrical, mechanical, and structural properties.

Structure and Microstructure

The physical properties are related to the intrinsic characteristics of the materials such as the purity or the microstructure. Hence the different phases present in the materials were characterized by x-ray diffraction (XRD) analysis using a Bruker D4 Endeavour diffractometer working with the K α ray of copper ($\lambda = 1.5418 \text{ \AA}$).

A scanning electron microscope JEOL JSM 6400, coupled with an energy dispersive spectroscopy (EDX) analyzer system, was used to determine the microstructure of the sample. The EDX analysis revealed the elemental composition of the specimen and checked the chemical homogeneity of the ceramic.

The densification corresponds to the ratio of the actual density of the substrate to the theoretical density. The density was determined from the weight and the dimensions of the samples.

Dielectric Strength

The dielectric strength (in kV/mm) is defined as the maximum electric field that a material is able to withstand before breakdown occurs. The equipment used to determine the dielectric strength involved a 25-L stainless-steel chamber, which may be resistively heated up to a 450°C ambient temperature, and which was able to withstand an internal pressure of 30 bar N $_2$ (to avoid flashback at the surface of the sample). The equipment allowed the application of voltages reaching 30 kV rms AC. The voltage was increased from zero to the maximum voltage value, or until breakdown occurred, at a uniform rate of rise of 2 kV/s. If no breakdown occurred, the voltage was maintained for 15 s and then decreased.

Mechanical Strength

The mechanical strength was assessed through the flexural strength (in MPa), measured by the three-point bending test at a crosshead speed of 5 mm/min. It was then calculated according to Eq. 1:

$$\sigma_{\text{breaking}} = \frac{3F \cdot L}{2 \cdot b \cdot e^2}, \quad (1)$$

where F (N) is the force applied until breaking occurs, L (m) is the span length ($L = 13 \text{ mm}$), b (m) is the width, and e (m) is the thickness of the sample.

Thermal Conductivity

Since the maximum temperature of the elementary semiconductor die directly influences the reliability of a semiconductor component, the thermal resistance has to be minimized to keep the temperature as low as possible.

The thermal conductivity (in W/m K) was measured using the hot disk method. To ensure the performance of the material at a working temperature of 300°C, which implies a component temperature that can reach values up to 400°C, the measurements were performed at temperatures from 25°C to 400°C (which corresponds to the highest temperature that the probe can withstand without damage).

Coefficient of Linear Thermal Expansion (CTE)

As shown by several studies, the thermomechanical strength determines the point of cracking of the ceramic or of the DBC.⁵ To avoid cracking, the difference between the CTE of all the different parts of the assembly must be kept as small as possible.

The change of length Δl induced by an increase of temperature ΔT defines the CTE as given by the following equation:

$\frac{\Delta l}{l_0} = \text{CTE} \cdot \Delta T$, where l_0 is the initial length. The unit for CTE is °C $^{-1}$.

The CTE was measured with a dilatometer (Netzsch 402E). The sample was submitted to a thermal treatment under a flow of air (80 cm 3 /min). The final temperature of 500°C was reached at a rate of 1°C/min.

Physicochemical Stability

The oxidation sensitivity was also studied by thermogravimetric analysis using a simultaneous symmetrical thermoanalyzer TAG 16 SETARAM. The thermal cycle is the same as that used for the determination of the CTE. A step of 24 h was added in some case as described in the following.

Thermal Shock Resistance

The thermal shock resistance (TSR) of a ceramic depends on its mechanical and thermal properties. The following ratio is used to compare test materials⁶:

$\text{TSR} \cong \sigma_r \cdot k/E \cdot \text{CTE}$, where σ_r is the flexural strength resistance, k is the thermal conductivity, E is Young's modulus, and CTE is the coefficient of thermal expansion.

RESULTS AND DISCUSSION

In this section, the microstructure and the structure of the materials are first presented. The physical properties are then reported and correlations proposed.

Microstructure

Secondary-electron imaging shows the morphology and the size of the grains. The chemical contrast is shown using backscattered electron imaging. This technique gives an idea of the homogeneity and, in some cases, the location of the secondary phases.

The observation of the surface of the alumina sample (Fig. 1) shows a bidisperse population of grains with diameters of $d_1 = 2 \mu\text{m}$ and $d_2 = 5 \mu\text{m}$. Some porosity can be seen (Fig. 1a') and was confirmed by the densification calculation for the plate that reached 95%. The chemical contrast micrograph shows the homogeneity of the substrate (Fig. 1b).

The same observations were performed on the two AlN substrates. Both AlN substrates in Figs. 2a and 3a show bidisperse populations with the same grain size ($\varnothing_1 = 1.5 \mu\text{m}$ and $\varnothing_2 = 5 \mu\text{m}$). In this case,

porosity is visually minimal (Figs. 2a' and 3a') and a high densification was determined (97% for AlN1 and 98% for AlN2). It is important to specify here that the theoretical density used to calculate densification corresponds to pure materials. However, considering the small volume fraction of the secondary phases, the error in the densification is low and so the difference of densification (1%) between AlN1 and AlN2 is significant.

The chemical contrast observations in Figs. 2b and 3b indicate the presence of a secondary phase (bright zone) containing atoms with a higher atomic number than those in the dark area. EDX analysis, run at 30 kV, confirms the presence of yttrium in these bright areas. Figure 4 also proves that aluminum nitride AlN2 contains a higher level of sintering aid (Y_2O_3).

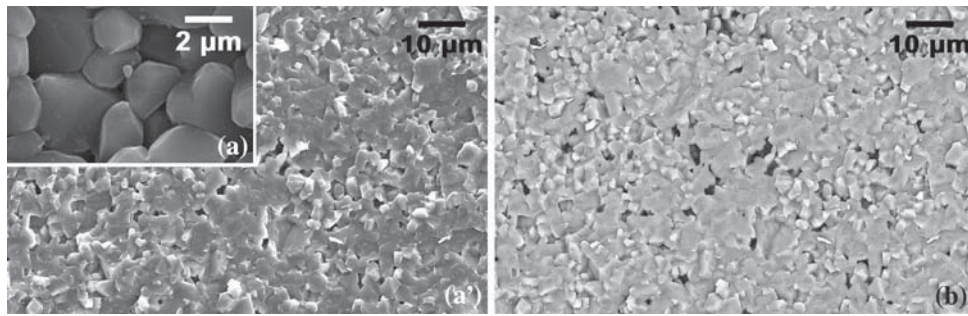


Fig. 1. Micrographs of Al_2O_3 substrates: (a) surface, (a') cross-section, and (b) chemical contrast on the cross-section.

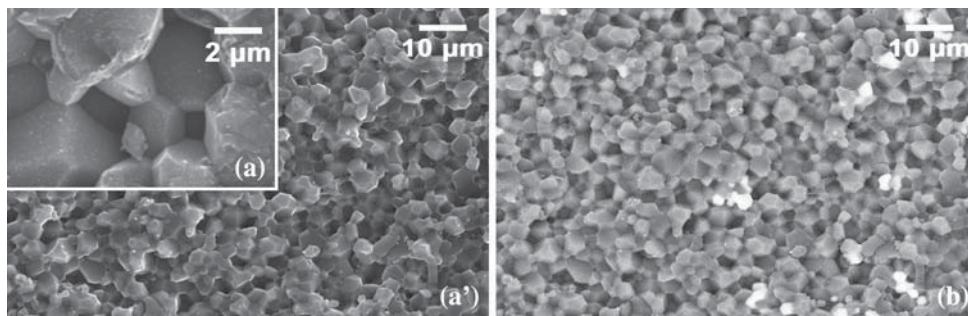


Fig. 2. Micrographs of AlN1 substrates: (a) surface, (a') cross-section, and (b) chemical contrast on cross-section.

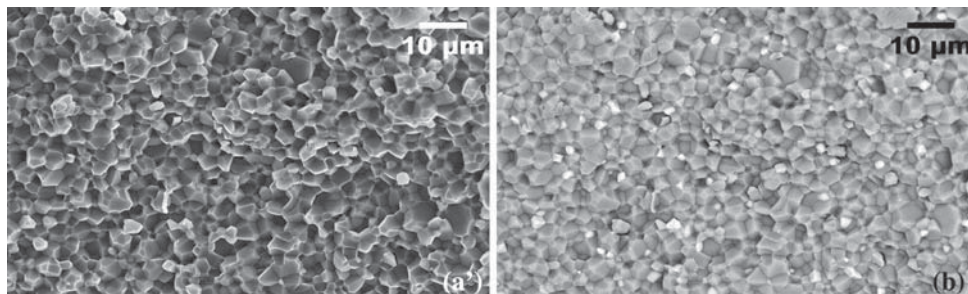


Fig. 3. Micrographs of AlN2 substrates: (a') cross-section and (b) chemical contrast on cross-section.

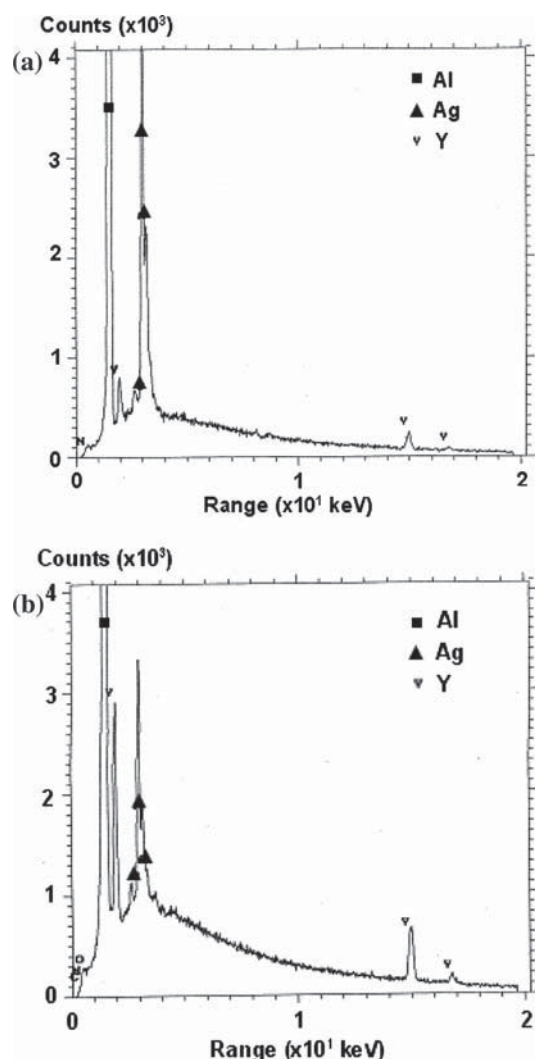


Fig. 4. EDX analysis of AlN substrates: (a) AlN1 and (b) AlN2.

The microstructures of the boron nitride substrates (Figs. 5 and 6) are quite different from the others. Both thicknesses studied presented a layered structure, and the grains showed a large size distribution. The observations made on the ceramic surface appear quite different. In the thicker plate

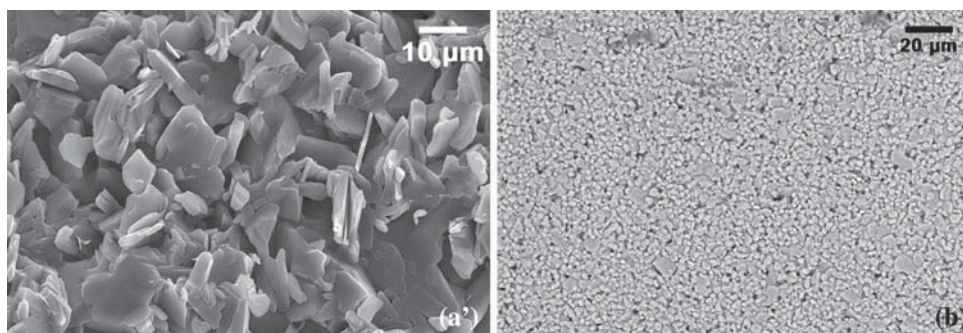


Fig. 5. Micrographs of BN thin substrates: (a') surface and (b) chemical contrast on edge.

(Fig. 6), the layer of particles seems to be parallel to the surface, probably because of the manufacturing process.

As seen in Figs. 5a' and 6a', the boron nitride substrates are not highly densified. The densification calculation confirmed these results, giving 55% densification for the thinner sample and 60% for the thicker one. The chemical contrast observations showed that the substrates were homogeneous.

According to the XRD patterns and bearing in mind that the limit of the XRD detection is about 2%, only the aluminum nitride samples appear to be multiphased. The diffraction patterns (Fig. 7a) show that the alumina was of the alpha type, crystallizing in the rhombohedral system (JCPDS 82-1399). The homogeneity observed in the chemical contrast observations is confirmed.

Figure 7b shows the presence of the hexagonal variety of boron nitride (JCPDS 34-0421) in both samples.

The diffraction patterns of the silicon nitride sample (Fig. 7c) show that this material crystallizes in the hexagonal system (JCPDS 71-0623).

Aluminum nitrides are clearly multiphase samples (Fig. 7d). As currently studied, sintering AlN without sintering aids is difficult. Therefore, Y_2O_3 is frequently used to optimize densification as well as for its impact on the thermal conductivity.⁷⁻¹⁰ In the conventional sintered AlN ceramics, the presence of Y_2O_3 as a sintering aid can lead to a thermal conductivity greater than 180 W/m K.

It is well known that the presence of Y_2O_3 leads to the precipitation of yttrium aluminates in the AlN sample. The nature of the phases depends on the amount of additive, as shown in Fig. 8. In the samples tested, two phases were found, in addition to AlN (Fig. 7d). The first one was $YAlO_3$, called yttrium aluminum perovskite (YAP) with an orthorhombic structure. The second one, detected in smaller amounts was $Y_4Al_2O_9$, called yttrium aluminum monoclinic (YAM). According to Ueno,¹¹ the amount of Y_2O_3 additive in the aluminum nitrides tested should be in the range of 3 wt.% to 4 wt.%.

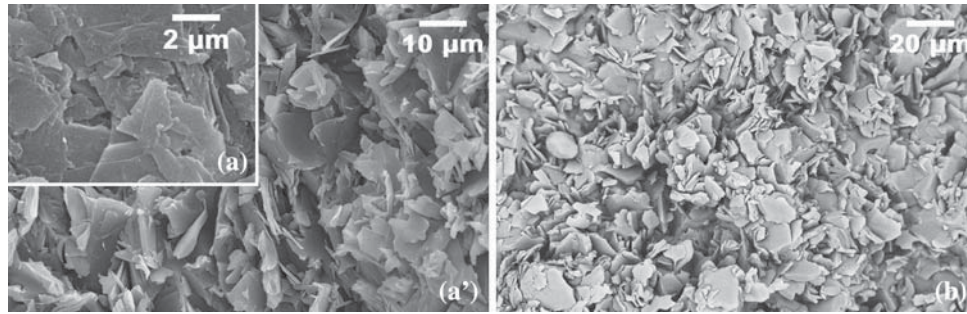


Fig. 6. Micrographs of BN thick substrates: (a) surface, (a') cross-section, and (b) chemical contrast on cross-section.

Dielectric Strength

The dielectric strength was determined from the measurement of five different samples of each material under study and calculated using Weibull statistics. In this article, only the values measured at room temperature and at 450°C are presented. The results are reported in Fig. 9. In these plots the Weibull value of the dielectric strength is given by the height of the box, and the whisker represents the distribution.

First, results at room temperature prove that all the materials presented here are suitable candidates as substrates in high-voltage power applications. In fact, their dielectric breakdown ranges from 20 kV/mm to more than 40 kV/mm, most presenting a dielectric strength higher than 30 kV/mm. On the other hand, it is also important to note that the value obtained on BN samples at room temperature is far from that claimed by the manufacturer (Table II). The poor densification explains this low value.

Regarding the measurements performed at high temperature, three main behavior types are observed: AlN2 presented a marked change in its dielectric strength, whereas the Al₂O₃, AlN1, and BN (small thickness) samples showed little or no changes. Si₃N₄ samples presented an increase of their dielectric strength with temperature. In all cases, the accuracy of the measurements was very high, emphasizing the homogeneity of the samples in a batch.

The dielectric strength of boron nitride remained relatively constant. The role of the binders for this material has already been underlined by some authors. Dagdag et al.¹² measured the dielectric properties of three types of boron nitride, respectively, with boric acid binder (as was the case for the sample tested in this paper), calcium borate binder, and the last without any additives. The measurements show that for the two last samples the dielectric strength was halved when the temperature reached 450°C. It may therefore be concluded that the use of boric acid as a binder ensures the stability of the electrical properties.

Finally, AlN substrates may or may not still be considered as valuable candidates depending on the

manufacturer. The first type (AlN from manufacturer 2) presented a dielectric strength (~40 kV/mm) with a lower distribution than at room temperature, while the dielectric strength of AlN from manufacturer 3 decreased dramatically down to an unsuitable value of 6.5 kV/mm.

Since the first type of AlN substrates seemed to present the best electrical characteristics, and in order to understand the behavior observed for both types of AlN samples, measurements were performed at different temperatures ranging from 25°C to 450°C (Fig. 10). For both manufacturers, the dielectric strength of AlN substrates remained constant or presented a slight increase for temperatures from room temperature up to 200°C. For higher temperatures, the dielectric strength of AlN2 samples decreased dramatically, whereas it remained constant for AlN1 samples. Whatever the mechanism explaining these changes, the plots highlight a sharp distribution of results, demonstrating that the manufacturing process is controlled and reproducible and is not responsible for the observed results.

Among the different possible causes the most likely is, as already mentioned, the influence of the type and level of binder. Many studies have already reported the influence of additives on the thermal conductivity. As reported in this article, it is also seen to influence the dielectric strength. A trade-off must therefore be found between thermal conductivity and dielectric strength.

Flexural Strength

The influence of the geometric dimensions of the sample on the flexural strength was evaluated by measurements performed on samples of different sizes (Table III). Since the length does not influence the mechanical strength (Eq. 1), a constant value of 20 mm was used. For all the tests, the temperature was 24°C and the relative humidity was 45%. It must first be noted that the width of the sample only influences the uncertainty of the measurements. Naturally, for a given material, the greater the thickness, the stronger the blank.

The mechanical strength of boron nitride samples was very low. This may be explained both by the

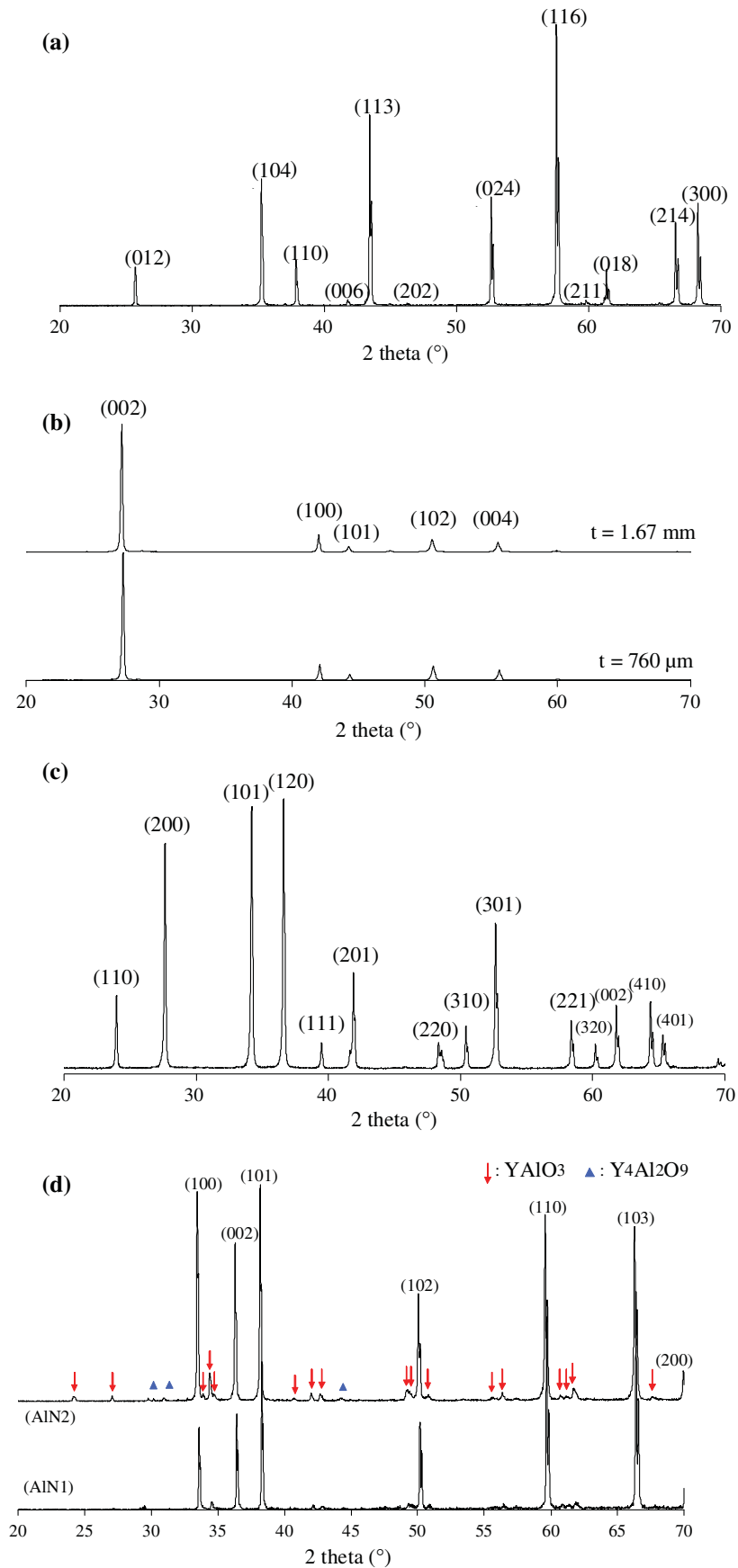


Fig. 7. XRD patterns: (a) alumina, (b) boron nitride (t = thickness), (c) silicon nitride, and (d) aluminum nitride.

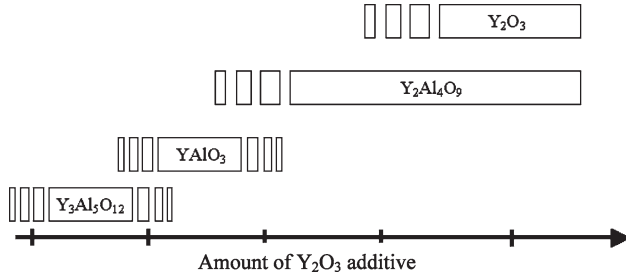


Fig. 8. Amount of yttrium aluminates versus amount of additive.

poor densification of the samples and by the particular platelet morphology, favoring the sliding of particles.

Regarding aluminum nitride samples, we found that the secondary phase had little or no influence on the mechanical resistance. Our values are in agreement with those provided by the supplier.

Thermal Conductivity

Except for boron nitride, the measured thermal conductivity was in good agreement with the supplier's values (Table IV).

The difference observed for boron nitride samples may again be attributed to the poor densification. The significant percentage of air trapped in the bulk along with its low conductivity ($k_{\text{air}} = 0.02 \text{ W/m K}$) led to a direct impact on the global conductivity of the material. On the contrary, and not surprisingly, aluminum nitride clearly showed the highest thermal conductivity. Many studies have already reported how the nature of the additive affects the secondary phases and the thermal properties of the material.

Lastly, since aluminum nitride substrates appear to be the most suitable candidates for high-temperature applications, the changes in its thermal conductivity with temperature are reported in Fig. 11.

The thermal conductivity of AlN decreased from 179 W/m K to 110 W/m K between room temperature and 300°C . The relative decrease ($\Delta k/k = 40\%$) is quite similar to that observed for alumina ($\Delta k/k = 35\%$.) Boron nitride exhibits a higher thermal conductivity than alumina, but it was

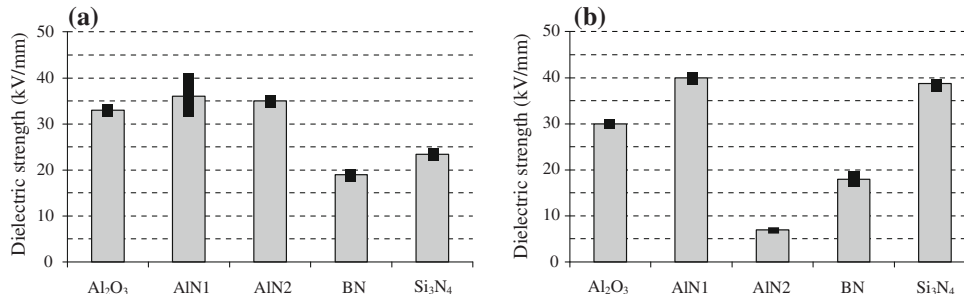


Fig. 9. Dielectric strength at (a) room temperature and (b) at 450°C .

Table II. Supplier's Value for the Dielectric Strength of Different Materials

	Supplier's Value (kV/mm)
Alumina Al_2O_3	10
Boron nitride BN	53
Aluminum nitride AlN1 (manufacturer 2)	16
Aluminum nitride AlN2 (manufacturer 3)	14
Silicon nitride	14

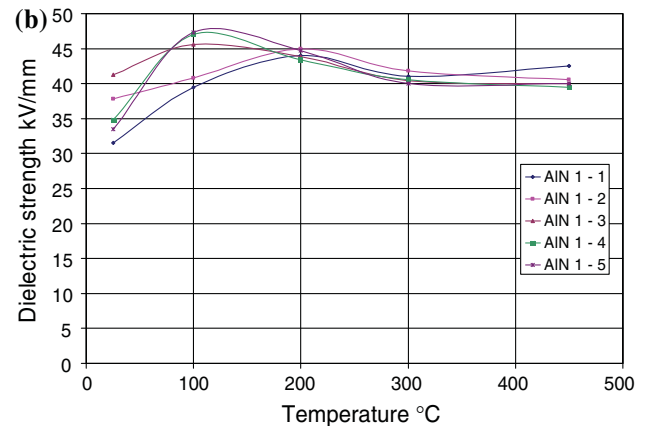
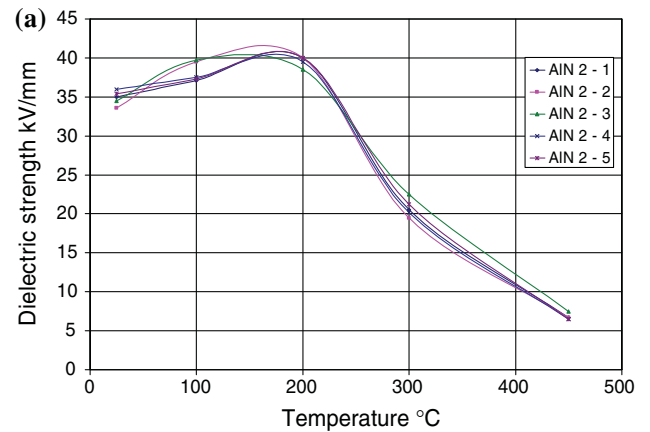


Fig. 10. Dielectric strength of (a) AlN2 and (b) AlN1 versus temperature.

Table III. Flexural Strength Measured at Room Temperature Versus Supplier's Values

	Samples Size (Width × Thickness) (mm)			Supplier's or Literature Values Flexural Strength (MPa)
	5–7 × 0.635	20 × 0.635	5–7 × 1.67	
	Measured Flexural Strength (MPa)			
Alumina	395 ± 100	377 ± 45	–	300–400 ^a
Boron nitride	18 ± 4	–	44 ± 5	76
Aluminum nitride AlN1	365 ± 73	–	–	360
Aluminum nitride AlN2	361 ± 92	–	–	300–360 ^a

^aWe report here the range of values found in the literature.

Table IV. Thermal Conductivity Measured at Room Temperature Versus Supplier's Values

Material	Thermal Conductivity (W/m K) at Room Temperature	Uncertainty (%)	Supplier's Values
Alumina	28.1	0.04	26–35 ^a
Boron nitride (BN thickness 2)	40.5	0.25	59
Aluminum nitride (AlN manufacturer 2)	175.0	0.72	170

^aWe report here the range of values found in the literature.

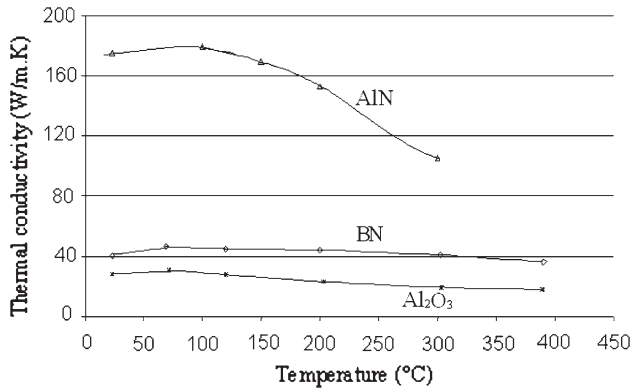


Fig. 11. Thermal conductivity of aluminum nitride, boron nitride, and alumina samples versus temperature.

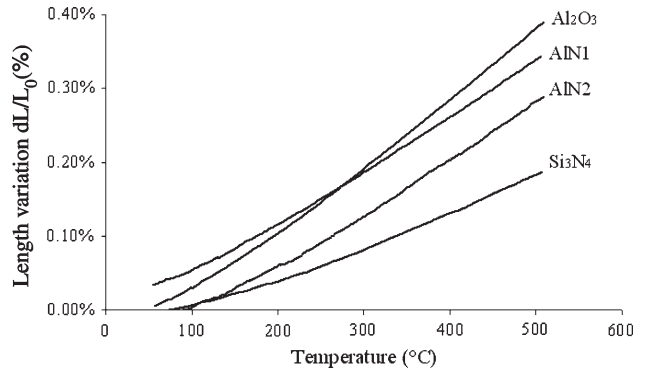


Fig. 12. Length changes of the substrates versus temperature.

nonetheless lower than that given by the supplier. However, aluminum nitride substrates still remain the best candidates.

Coefficient of Thermal Expansion

The CTEs were evaluated in the range 20°C to 500°C from the slopes of the curves of length variation versus temperature (Fig. 12). The values are reported in Table V. Three measurements were carried out for each sample to determine the uncertainty (Table VI).

For boron nitride samples, the variation of length versus temperature was not linear even after heat treatment was used to release the water. Therefore, we were unable to determine the CTE for BN.

In the other cases, the CTE determined here was slightly higher than the nominal value. The CTE of

Table V. Thermal Coefficient of Expansion Measured at Room Temperature Versus Supplier's Values

	CTE (10 ⁻⁶ /°C)	Supplier's Values
Alumina	9.1 ± 0.3	6.8–9
Boron nitride	–	6
Aluminum nitride AlN1	6.6 ± 0.5	5.2
Aluminum nitride AlN2	7.0 ± 0.7	4.4–6.2
Silicon nitride	4.54 ± 0.7	3.1

aluminum nitride and of silicon nitride samples presented the best match with the other parts of the stack and in particular with the semiconductor devices and particularly with the SiC components.

Table VI. Overall Characteristics of the Different Substrates under Study

	Al ₂ O ₃	BN	AlN1	AlN2	Si ₃ N ₄
Chemical stability	+	-	+	+	+
Dielectric strength	+	-	+	+	
stability	+	+	+	--	
Flexural strength	+	--	+	+	(++)
Thermal conductivity	-	-	++	++	(-+)
stability	-	+	-	-	
CTE	-		+	+	++
TSR	-	-	+	+	+
Cost	+	-	-	-	--

++: very good; +: good; -+: not too bad; -: poor; --: unacceptable.

Physicochemical Stability

The stability of the different samples was evaluated from the mass changes during thermal cycling under air flow. The results are reported in Fig. 13 for boron nitride samples and in Fig. 14 for alumina and aluminum nitride samples.

Boron nitride presents a mass loss thought to be due to water release, the material being hygroscopic. Alumina, aluminum nitrides, and silicon nitride materials all exhibit a very small

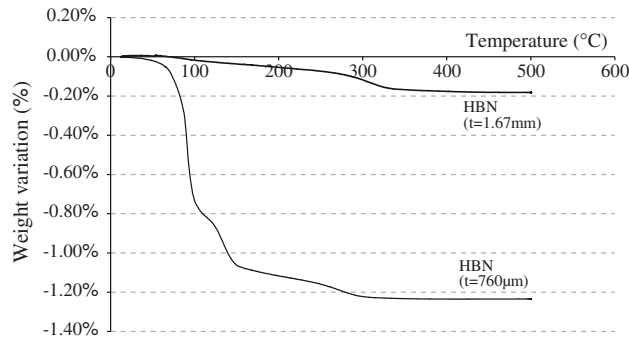


Fig. 13. Weight variation of boron nitride samples versus temperature.

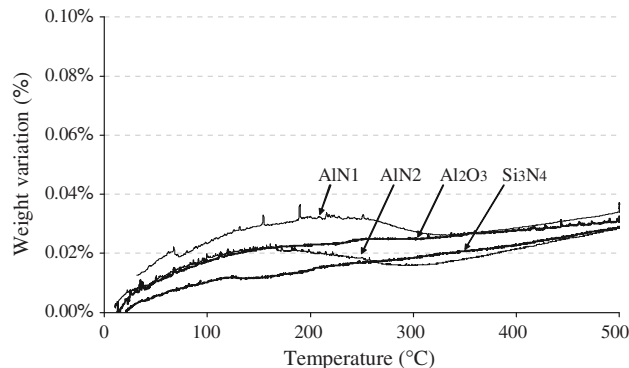


Fig. 14. Weight variation of alumina, aluminum nitride, and silicon nitride samples versus temperature.

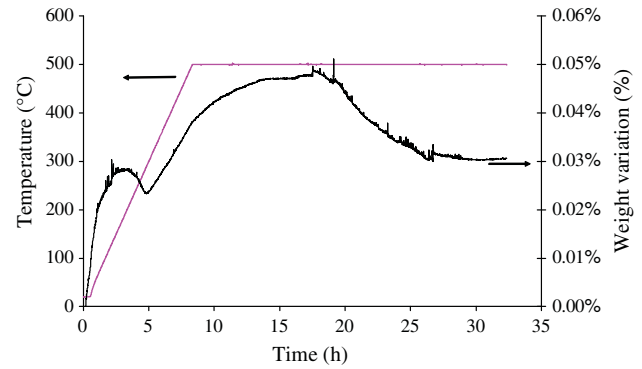


Fig. 15. Weight variation of sample AlN1 versus time at 500°C.

mass variation (<0.04%) between room temperature and 500°C, thus confirming their stability. Lastly, to ensure long-term stability, a sample of aluminum nitride AlN1 was maintained at 500°C for 24 h and its mass variation followed (Fig. 15). After a weight increase of up to 0.05% during the first 5 h, there was a decrease and a stabilization giving a net variation of 0.03% (which is negligible).

CONCLUSION

In order to compare the different substrates under study, their main characteristics are summarized in Table VI reporting the pros and cons for each substrate. Hence, boron-nitride-based substrates must be eliminated for the targeted applications. The poor densification of the materials under study leads to poor mechanical properties. AlN as the base material of DBC substrates combines both excellent thermal conductivity and high mechanical stability. Another advantage of AlN compared with alumina is its CTE, which is closer to that of silicon and silicon carbide, resulting in less stress in the power semiconductor devices and on the solder joint during thermal cycling.

REFERENCES

1. W. Wondrak, *Microelectron. Reliab.* 39, 1113 (1999). doi:10.1016/S0026-2714(99)00158-4.
2. M. Pecht, P. Lall, and E.B. Hakim, *Qual. Reliab. Eng. Int.* 8, 167 (1992). doi:10.1002/qre.4680080304.
3. P.L. Dreike, D.M. Fleetwood, D.B. King, D.C. Sprauer, and T.E. Zipperian, *IEEE Trans. Compon. Packag. B* 17, 594 (1994).
4. P. McCluskey, D. Das, J. Jordan, L. Condra, R. Gryzbowski, T. Torri, and J. Fink, *Adv. Microelectron.* 25, 19 (1998).
5. J.V. Manca, W. Wondrak, W. Schaper, K. Croes, J. D'Haen, W. De Ceuninck, B. Dieval, H.L. Hartnagel, M. D'Olieslaeger, and L. De Schepper, *Microelectron. Reliab.* 40, 1679 (2000). doi:10.1016/S0026-2714(00)00187-6.
6. W.D. Callister Jr., *Science et Génie des Matériaux*, 5th ed. (Paris: DUNOD, 2003).
7. M. Okamoto, H. Arakawa, M. Oohashi, and S. Ogihara, *J. Ceram. Soc. Jpn.* 97, 1486 (1989).
8. A.V. Virkar, T.B. Jackson, and R. Cutler, *J. Am. Ceram. Soc.* 72, 2031 (1989). doi:10.1111/j.1151-2916.1989.tb06027.x.
9. M. Hirano, K. Kato, T. Isobe, and T. Hirano, *J. Mater. Sci.* 28, 4725 (1993). doi:10.1007/BF00414264.

10. M. Kasori and F. Ueno, *J. Eur. Ceram. Soc.* 15, 435 (1995).
doi:[10.1016/0955-2219\(95\)91432-N](https://doi.org/10.1016/0955-2219(95)91432-N).
11. F. Ueno, *Electric Refractory Materials*, ed. Y. Kumashiro (New York: Marcel Dekker, Inc., 2000), p 699.
12. S. Dagdag, T. Lebey, D. Dinculescu, M.-L. Locatelli, and E. Dutarde, *IEEE Int. Conf. Electron. Mater. Packag.* 8, 1 (2006).